

Interactive Point Set Joint Registration and Co-segmentation

ID: paper1049

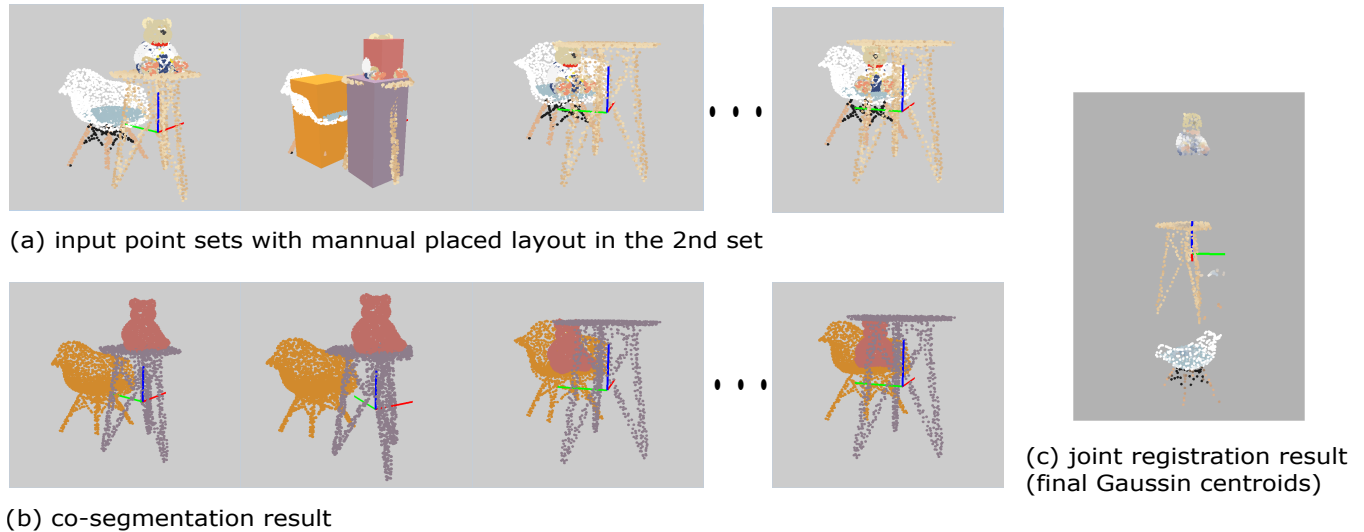


Figure 1: (a) are input point sets and user have initialized layout for the 2nd set by interactively placing boxes in it. (b) are result of co-segmentation. (c) are the Gaussian centroids in three groups (from top to down) corresponding to three objects

Abstract

We present a method of joint registration and co-segmentation for point sets of objects. We view the joint registration and co-segmentation as two problems heavily entangled with each other. To model such entangled problems, we treat the input point sets as samples from a generative model and bring up with a novel formulation based on Gaussian mixture model. By maximizing the posterior probability of the samples, we gradually recover the latent object model and object level segmentation and align the objects to the latent model(solve the registration). Along with the formulation, we design a procedure of interaction that can help users to intuitively initialize the optimization. Our evaluation shows that our novel method is helpful and effective to do the joint registration and co-segmentation on point sets of multiple objects.

Categories and Subject Descriptors (according to ACM CCS): I.3.8 [COMPUTER GRAPHICS]: Applications—I.4.8 [IMAGE PROCESSING AND COMPUTER VISION]: Scene Analysis—Range data

1. Introduction

In many researches and applications of indoor scenes the data of segmented and even annotated 3D indoor scenes are required as either data base or training data (e.g. [NXS12] [DSS12] [FRS*12] [CLW*14] [FSL*15]).

One way to build such database is to interactively compose scenes

from 3D shape models resulting in scenes with object segmentation and annotation naturally available, or to manually segment and annotate existing scenes. This procedure can be tedious and time consuming, despite the efforts to improve the interaction experience(e.g. [MSL*11] [XCF*13]).

Another way is to automatically generate scenes from 3D shape models according to the input RGB or RGB-D images(e.g.

[LZW^{*}15] [CLW^{*}14]). In such methods, a retrieval procedure is usually needed and inevitably limit the result to a certain set of 3D models despite the actual 3D model in the input images.

We prefer an approach that helps us build such dataset directly from the captured data. One of the major gap between the required data set and available scene capturing framework (e.g. [IKH^{*}11]) is the general object level segmentation. We want to stress that a general object level segmentation problem should not be treated as an equivalence of multilabel classification problem since it is not limited to a certain set of objects. For 3D data, [JGSC15] used some simplified physical prior knowledge (i.e. the block-based stability) to help achieving the general objectness segmentation, while the work of [XHS^{*}15] proposes a practical and rather complete framework to close the gap between the required data set and available scene capturing method. One of the observation in [XHS^{*}15] is that the motion consistency of rigid object can serve as a strong evidence of general objectness. To exploit this fact, they employ a robot to do proactive push and use the movement tracking to verify and iteratively improve their object level segmentation result. Our work presented in this paper is trying to exploit the same observation from a different approach.

We intend to use the motion consistency in objects that is naturally revealed by human activities along the time. Down to this approach, we are facing the choice of scanning scheme. One way is to record the change of the scene along with the human activities, another is to schedule a daily or even a once every half day sweep to only record the result of human activities but avoid the instant of human motion. The main challenge brought in by the second scheme is that we may not be able to solve the object correspondence by a local search due to the sparse sampling over time, but the very same challenge exists in the first scheme due to the exclusion caused by human bodies not to mention other additional process(e.g. tracking with severe occlusion) needed for human bodies. With the second scanning scheme, our original intention of building 3D scene data set from capturing naturally leads us to the problem of coupled joint registration and co-segmentation.

In this problem, registration and segmentaion are entangled in each other. On one hand the segmentation depends on the registration to connect the point clouds into series of rigid movement so that the objectness segmentation can be done based on the motion consistency, on the other hand, the registration depends on the segmentation to break the problem into a series of rigid joint registration instead of a joint registration with non-coherent point drift(A pair of points is close to each other in one point set but their correspondent pair of points in another point set is far from each other, in other words, the point drift of this pair is non-coherent. (This happens when this pair of points actually belong to different objects.) To model the problem, we employ a group of Gaussian mixture models and each of these Gaussian mixture models represents a potential object. This model unentangle the registration and segmentation in the way that the segmentation can be done by evaluate the probability of points belongs to the Gaussian mixture models and the registration can be done by evaluate rigid registration against each gaussian mixture models.

In summary our work makes following contributions:

Firstly, as far as we know we are the first work that bring up with the problem of point set joint registration and co-segmentation for indoor scenes.

Secondly, we come up with a Gaussian mixture model based formulation to simultaneously model both the joint registration and co-segmentation problem.

Thirdly, targeting the disadvantages of our formulation, we design a procedure of interaction and provide a practical tool for point set joint registration and co-segmentation based on it. We will release our tool with acceptance of this paper.

2. Related Work

In this section we explain how our work is related to the previous works and how we draw experience from these previous works.

2.1. Point Set Registration with GMM Representation

There are a series of work that uses gaussian mixture model as representation for point set to formulate the registration problem. [MS10] consider the registration of two point sets as a probability density estimation problem. They force the Gaussian mixture model centroids to move coherently as a group to preserve the topological structure of the point sets. Their method is applicable to both rigid registration and non-rigid registration. As we highlighted in Section 1, our problem is different from the non-rigid registration considered in [MS10], the point drift could be non-coherent in our probelm. [JV11] summarized the works for point set registration using Gaussian mixture models and present a unified framework for the rigid and nonrigid point set registration problem. These works select one of the point set as the “model”. Unlike these works, [EKBHP14] treats all the point sets as data: they are all realizations of a Gaussian mixture and the registration is cast into a clustering problem. Comparing to these works, our work is most related to [EKBHP14]. Our formulation can be seen as an extention of the formulation of [EKBHP14] to simultaneously handle joint registration and co-segmentation.

2.2. Image segmentation and co-segmentation

[RKB04] is an influential work for interactive image segmentation. It uses two Gaussian mixture model, one for foreground and one for background. To initialize these two Gaussian mixture models, [RKB04] let users place a rectangle that contain the foreground. Our design of interaction draw on the experiance from [RKB04]. The difference is that our interaction is designed for 3D space and can handle multiple objects segmentation rather than foreground-background segmentation. [TSS16] jointly recover cosegmentation and dense per-pixel correspondence in two images. Its cosegmentation is limited to foreground-background segmentation. Our work solve a similar problem for multiple 3D point sets.

2.3. Segmentation from Motion

The idea that motion can be strong hint for segmentation is used in many works. [XHS^{*}15] employs a robot to do proactive push and track the motion to learn object segmentation. [LPR^{*}16] exploit the motion in video and use the motion edge as training data to learn an edge detector for image. These methods lean on the motion that is continuous in time and can be tracked. Our method can handle motion that is not continuous in time.

2.4. 3D Object Recognition based on Correspondence Grouping

By allowing interactively input layout, the joint registration and co-segmentation problem can be treated as a series of 3D object recognition problem in point sets. Our method should be seen as one of the correspondence grouping method. Comparing to the previous methods of [TS10] and [CB07], our method simultaneously solve the problem for multiple target models in multiple scenes.

3. Method Overview

3.1. Problem Statement

Given M point sets with I_m points $V_m = \{v_{mi}\}$ for the m^{th} point set (Figure 1 (a) shows an example of input point sets.), we intend to simultaneously partition the point sets into N objects and find the rigid transformations $\{\phi_{mn}(x) = R_{mn}x + t_{mn}\}$ that transform each object model to its observed position in each input point set. For partition, we output point-wise label vectors $\{y_m\}$ for each input point set to indicate its object partition. (Figure 1 (b) illustrates result label vectors by assigning same color to points with same label.)

Symbol	Meaning
V	The input point sets.
V_m	The m^{th} input point set.
v_{mi}	The i^{th} point of V_m .
z_{mi}	The latent parameter for v_{mi} .
$z_{mi} = k$	means v_{mi} is generated by k^{th} Gaussian
Z	$Z = \{z_{mi} m=1...M, i=1...I_m\}$
K_{all}	The total number of Gaussian models.
K_n	The number of Gaussian for n^{th} object. $\sum_n^K K_n = K_{all}$
p_k	The weight of k^{th} Gaussian. $\sum_k^K p_k = 1$
x_k	The centroid of k^{th} Gaussian.
Σ_k	The covariance matrix of k^{th} Gaussian.
σ_k	$\Sigma_k = \sigma_k^2 I$. (I is identity matrix here.)
ϕ_{mn}	Transformation from n^{th} object to m^{th} input set.
R_{mn}	The rotation matrix for ϕ_{mn} .
t_{mn}	The translation vector for ϕ_{mn} .

Table 1: Table of Symbols Used in the Paper

3.2. Basic Formulation

To establish our formulation, we first define symbols as in Table ???. To simultaneously model the joint registration and co-segmentation, we come up with a generative model as follows:

$$P(v_{mi}) = \sum_{k=1}^{K_n} p_k \mathcal{N}(v_{mi} | \phi_{mn}(x_k), \Sigma_k) \quad (1)$$

which treat the i -th observed point v_{mi} from the m -th point set as a sample point generated by one of N object models. Each object model is represented by a group of K_n gaussian models.

The model parameters are:

$$\Theta = \{\{p_k, x_k, \Sigma_k\}_{k=1}^{K_n}, \{\phi_{mn}\}_{m=1, n=1}^{MN}\}$$

In order to find the parameters that fit the input data, Our goal of optimization is to maximize the probability of observed input sets sampled from the latent model. This problem can be solved in the framework of expectation-maximization. In particular, we bring in a latent parameter

$$Z = \{z_{mn}|m = 1...M, n = 1...N_m\}$$

such that $z_{mn} = k (k = 1... \sum K_n)$ assigns the observed point v_{mi} to the k -th component of Gaussian mixture model. We aim to maximize the expected complete-data log-likelihood:

$$\epsilon(\Theta|V, Z) = \mathbb{E}_Z [\ln P(V, Z; \Theta)|V] = \sum_Z P(Z|V, \Theta) \ln P(V, Z; \Theta) \quad (2)$$

Such formulation can be seen as an adaption of joint registration formulation in [EKBHP14], upon which we separate Gaussian models into groups to express multiple objects and the latent parameter Z that assign observed points to gaussian models can naturally indicate the object level segmentation.

By the assumption of independent and identically distributed of input points, we can write the objective to:

$$\Theta = \arg \max \sum_{mik} \alpha_{mik} (\ln p_k + \ln P(v_{mi}|z_{mi} = k; \Theta)) \quad (3)$$

where $\alpha_{mik} = P(z_{mi} = k|v_{mi}; \Theta)$

By bringing in equation 1 and ignoring constant terms, we can rewrite the objective as:

$$\Theta = \arg \max \sum_{mik} \alpha_{mik} (\|v_{mi} - \phi_{mn}(x_k)\|_{\Sigma_k}^2 + \ln |\Sigma_k| - 2 \ln p_k) \quad (4)$$

where the $\|\cdot\|$ denotes the determinant and $\|x\|_A^2 = x^T A^{-1} x$. It is predefined that x_k is one of the gaussian centroid used to represent n -th object, which is why we apply transformation ϕ_{mn} on to the x_k . For the convenience of computation, we restrict the model to isotropic covariances, i.e., $\Sigma_k = \sigma_k^2 I$ and I is the identity matrix. Now, we can optimize this through iterating between estimating α_{mik} (Expectation-step) and maximizing $f(\Theta|V, Z)$ sequentially with respect to each parameters in Θ (Maximization-steps). These steps are:

E-step: this step estimates the posterior probability α_{mik} of v_{mi} to be a point generated by the k -th Gaussian model.

$$\alpha_{mik} = \frac{p_k \sigma_k^{-3} \exp(-\frac{1}{2\sigma_k^2} \|v_{mi} - \phi_{mn}(x_k)\|^2)}{\sum_s^K p_s \sigma_s^{-3} \exp(-\frac{1}{2\sigma_s^2} \|v_{mi} - \phi_{mn}(x_s)\|^2)} \quad (5)$$

M-step-a: this step update the transformations ϕ_{mn} that maximize $f(\Theta)$, given instant values for α_{mik} , x_k , σ_k . We only consider rigid transformations, making $\phi_{mn}(x) = R_{mn}x + t_{mn}$. The maximizer R_{mn}^*, t_{mn}^* of $f(\Theta)$ is the same with the minimizers of the following constrained optimization problems:

$$\left\{ \begin{array}{ll} \min_{R_{mn}, t_{mn}} & \|(W_{mn} - R_{mn}X_n - t_{mn}\mathbf{e}^T) \Lambda_{mn}\|_F^2 \\ \text{s.t.} & R_{mn}^T R_{mn} = I, |R_{mn}| = 1 \end{array} \right. \quad (6)$$

where Λ_{mn} is $K_n \times K_n$ diagonal matrix with elements $\lambda_{mnk} = \frac{1}{\sigma_k} \sqrt{\sum_i^{I_m} \alpha_{mik}} I_m$ is the number of point for the m -th input point set, $X_n = [x_1, x_2, \dots, x_{K_n}]$ is the matrix stacked by the centroids of gaussian models that are predefined to represent the n -th object.

\mathbf{e}^T is a vector of ones, $||\cdot||_F$ denotes the Frobenius norm, and $W_{mn} = [w_{m1}, w_{m2}, \dots, w_{mk}, \dots, w_{mK_n}]$, in which w_{mk} is a weighted point as:

$$w_{mk} = \frac{\sum_{i=1}^{I_m} \alpha_{mik} v_{mi}}{\sum_{i=1}^{I_m} \alpha_{mik}} \quad (7)$$

This problem have a similar solution of in [EKBHP14]. The only difference is that we are estimating the transformation from latent models to the input point sets instead of the transformation from input point sets to latent models, since there are multiple group of x_k corresponding to multiple objects in our latent model. The optimal can be given by:

$$R_{mn}^* = U_{mn} C_{mn} V_{mn}^T \quad (8)$$

$$t_{mn}^* = \frac{1}{tr(\Lambda_{mn}^2)} (W_{mn} - R_{mn} X_n) \Lambda_{mn}^2 \mathbf{e} \quad (9)$$

where $[U_{mn}, S, V_{mn}] = svd(W_{mn} \Lambda_{mn} P_{mn} \Lambda_{mn} X_{mn}^T)$ and $P_{mn} = I - \frac{\Lambda_{mn} \mathbf{e} (\Lambda_{mn} \mathbf{e})^T}{(\Lambda_{mn} \mathbf{e})^T \Lambda_{mn} \mathbf{e}} I$ is identity matrix. $C_{mn} = diag(1, 1, |U_{mn}| |V_{mn}|)$.

M-step-b: this step we update the parameters related to the Gaussian mixture model.

$$x_k^* = \frac{\sum_{m=1}^M \sum_{i=1}^{I_m} \alpha_{mik} (R_{mn}^{-1} v_{mi} - t_{mn})}{\sum_{m=1}^M \sum_{i=1}^{I_m} \alpha_{mik}} \quad (10)$$

where x_k is one of the Gaussian centroids that is predefined to represent n-th object.

$$\sigma_k^{*2} = \frac{\sum_{m=1}^M \sum_{i=1}^{I_m} \alpha_{mik} ||(v_{mi} - t_{mn} - R_{mn}^* x_k^*)||_2^2}{3 \sum_{m=1}^M \sum_{i=1}^{I_m} \alpha_{mik}} \quad (11)$$

$$p_k^* = \frac{\sum_{m=1}^M \alpha_{mik}}{M} \quad (12)$$

3.3. Bilateral Formulation

When considering point-wise features, we can add bilateral terms into the generative model.

$$P(v_{mi}; f_{mi}) = \sum_{k=1}^{K_n} p_k N(v_{mi} | \phi_{mn}(xv_k), \sigma v_k) N(f_{mi} | xf_k, \sigma f_k) \quad (13)$$

where f_{mi} is the feature vector for point v_{mi} and xf_k is the feature vector for k-th point in latent model. As shown in the formulation, there is no transformation applied onto xf_k , which means that this formulation is only suitable to the features that is rotation and translation invariant. For example, the point color vector $[red_{mi}, green_{mi}, blue_{mi}]$ is a suitable feature for this formulation. In this formulation $N(v_{mi} | \phi_{mn}(xv_k), \sigma v_k)$ is the spatial term and $N(f_{mi} | xf_k, \sigma f_k)$ is the feature term. For the bilateral formulation, iteration steps will be as follows:

E-step: in this step the calculation of posterior probability need to consider both the spatial term and the feature term.

$$\alpha_{mik} = \frac{p_k P_v(v_{mi}, \phi_{mn}(xv_k), \sigma v_k) P_f(f_{mi}, xf_k, \sigma f_k)}{\sum_s^K p_s P_v(v_{mi}, \phi_{mn}(xv_s), \sigma v_s) P_f(f_{mi}, xf_k, \sigma f_s)} \quad (14)$$

where $P_v(x, y, \sigma) = \sigma^{-3} \exp(-\frac{1}{2\sigma^2} ||x - y||^2)$ and $P_f(x, y, \sigma) = \sigma^{-D(x)} \exp(-\frac{1}{2\sigma^2} ||x - y||^2)$ and $D(x)$ means the dimension of the vector x .

M-step-a: for bilateral formulation, this step is the same with the basic formulation and the update can be done as (8) and (9).

M-step-b: for bilateral formulation, this step need not only update model centroids and variance for spatial term as (10) and (11), but also update the centroids and variance for feature term as in (15) and (16)

$$x f_k^* = \frac{\sum_{m=1}^M \sum_{i=1}^{I_m} \alpha_{mik} f_{mi}}{\sum_{m=1}^M \sum_{i=1}^{I_m} \alpha_{mik}} \quad (15)$$

$$\sigma f_k^{*2} = \frac{\sum_{m=1}^M \sum_{i=1}^{I_m} \alpha_{mik} ||(f_{mi} - x f_k^*)||_2^2}{D(f) \sum_{m=1}^M \sum_{i=1}^{I_m} \alpha_{mik}} \quad (16)$$

where $D(f)$ is the dimension of feature vectors.

The update of p_k for bilateral formulation is the same as the basic formulation in (12).

3.4. Interaction Design

Unfortunately, there are a large number of parameters that can not be easily initialized in our formulation. In this subsection we first introduce our design of interaction, which is intuitive for users to input the semantic prior this way. We then explain how we can easily initialize those parameters for our optimization based on the manual input.

As demonstrated in Figure 2, we let user choose one of the point sets and placing and editing boxes in it to indicate the layout for this point set. From this, we can easily initialize the total number of objects N and determine $\{K_n\}$ which is the numbers of Gaussian mixture models used to represent each object. These two pareme-

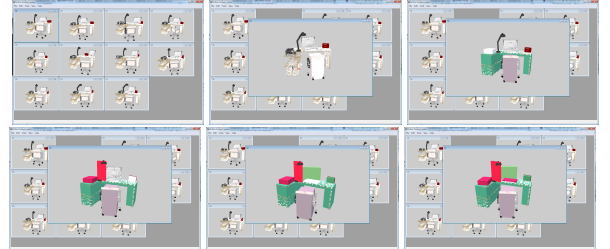


Figure 2: From the first to the ninth, the nine images show the procedure of interaction: the user pick one point set and place boxes in it to indicate the layout for this point set. The box in white is the box currently under editing. The boxes in other colors are boxes placed to represent object layouts. One color represent one object. The interaction allows multiple boxes to represent same object.(e.g. the desk is represented by three boxes in same color)

ters are difficult to be initialized without semantic prior, but with the input of the users we can naturally initialize the N as the number of different color label and the K_n as

$$K_n = \frac{V_n}{\sum V_n} K_{all} \quad (17)$$

in which the V_n represent the total volume of the boxes in the n-th color and the K_{all} is initialized as $K_{all} = \frac{\text{median}(I_m)}{2}$ and $\{I_m\}$ are point numbers of M input point set. This is an emperical choice borrowed from [EKBHP14].

The expectation maximizaton framework is easily converge to a local optimal. To cope with this problem we further use this layout (boxes) from interaction as a soft constraint to guide the optimization. Such constraint is enforced by simply altering the posterior probability α_{mik} as

$$\alpha_{mik}^* = \frac{\alpha_{mik}\beta_{mik}}{\sum_{i,k} \alpha_{mik}\beta_{mik}} \quad (18)$$

where the β_{mik} is the prior probability according to the boxes. It is defined as:

$$\beta_{mik} = \begin{cases} 1 & v_{mi} \in B_n \\ \exp(-\frac{\min_{v_{mj}} ||v_{mi} - v_{mj}||_2^2}{L}) & v_{mi} \notin B_n \text{ and } v_{mj} \in B_n \end{cases} \quad (19)$$

where the B_n is a point set that is enclosed by the boxes used to represent the layout of n-th object. The k-th Gaussian model is pre-defined to be one of the Gaussians used to represent n-th object. $\min_{v_{mj}} ||v_{mi} - v_{mj}||_2^2$ is actually the squared euclidean distance from point v_{mi} to the point set B_n , as we define the distance from a point to a point set as the minimum distance from the point to any point inside the point set. L here is a constant number with $L = 2r^2$, and r is the meadian of the radius of input point sets. The radius of a input point set is half of length of diagonal line of its axis aligned bounding box. This alteration on posterior probability is only done

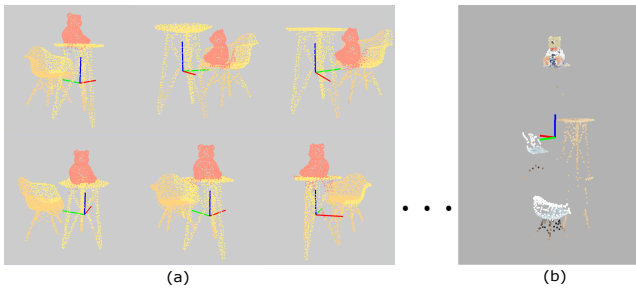


Figure 3: This figure shows an example result when converges to a local optimal. (a) is the result of segmentation of this local optimal. (b) is the final centroids of latent model. It shows that from top to down the 2nd and 3rd object model both include part of the table and part of the chair.

with the probability related to the m-th point set that have the manual input layout (the boxes) in it. This alteration can help prevent the optimization from converging to a local optimal as in Figure 3. The result from the Figure 3 have the same input and initialization with the result from Figure 1, but it doesn't use the posterior alteration as a soft constraint.

4. Algorithms and Implementation Details

In this section, we summarize the entire algorithm and explain the implemented details.

4.1. Algorithm

Based on our formulation in section 3, our algorithm can be summarized as in Algorithm 1.

Algorithm 1 Joint Registration and Co-segmentation (JRCS)

Input:

$\{V_m\}$: M input 3D point sets

Θ^0 : Initial parameters

$\{\beta_{ik}\}_m$: layout based prior

Output:

Θ^q : Final parameters

1. repeat

2. $q \leftarrow 0$

3. E-step: Use Θ^{q-1} to estimate α_{mik}^q according to (5) ((14) if use bilateral formulation)

4. alter α_{mik}^q with $\{\beta_{ik}\}_m$ according to (18)

5. M-step-a: Use $\alpha_{mik}^q, x_k^{q-1}$ to estimate $\{R_{mn}^q\}$ and $\{t_{mn}^q\}$ according to (8)(9)

6. M-step-b: Use $\alpha_{mik}^q, \{R_{mn}^q\}$ and $\{t_{mn}^q\}$ to other parameters for Gaussian models according to (10)(11)(12)

7. $q \leftarrow q + 1$

8. until Convergence

9. return Θ^q

4.2. Implementation Details

Initialization of Θ :

We first determine the total number of Gaussian model K_{all} as we explained in subsection 3.4. We set $p_k = \frac{1}{\sum K_n}$ which means each Gaussian model have the same weight at the beginning. We separate the Gaussian models into N groups to represent N objects. Each group has K_n Gaussian models based on (17). $\{x_k\}_n$ are Gaussian centroids of n-th group and they are initialized as a random positions uniformly distributed on the surface of a sphere. The radius of the sphere is chosen as the median of the radius of the input point sets r . The center of the n-th spheres is $c_n = (0, 0, z_n)$, where $z_n \in \{-(N-1)r, -(N-3)r, \dots, (N-1)r\}$. This means that the object models are vertically arranged in latent space as shown in Figure 1(m)(n) and in Figure 3(b). We choose vertical arrangement for latent model space merely for the convenience for the We choose the sphere as the initial shape so that we can initialize all the R_{mn} to identity matrix. For the t_{mn} we initialize them as $t_{mn} = -c_n$ so that all the object model starting with position at origin point when they are transformed to the space of each input set. However, if the m-th input point set has the manually placed layout, we treat the associated t_{mn} differently. For this case we have:

$$t_{mn} = \frac{\sum_{v_{mi} \in B_n} v_{mi}}{N(B_n)} - c_n \quad (20)$$

where $N(B_n)$ is the number of element in B_n and B_n is the point set that is enclosed by the manual input layout (boxes).

4.3. Hot Intervention Mechanism

Our current implementation of optimization is quite slow (fail to converge in iterative time) especially when the point numbers inside each input point set are large and it is possible for our optimization to stuck in a local optimal, requiring the guide from the manual input. As a compensation for these drawbacks. We implement a hot intervention mechanism, allowing the manual input take effect even after the optimization has started. Theoretically, this is possible due to the i.i.d assumption. This assumption makes it possible for the calculation of posterior probability being independent for each input point set. Even after the optimization is started, we can still allow the user to add more layouts for other point sets and the program can do the same alteration as (18) in the next iteration. The Figure 4 shows how the users can use the hot intervention mechanism with our tool.

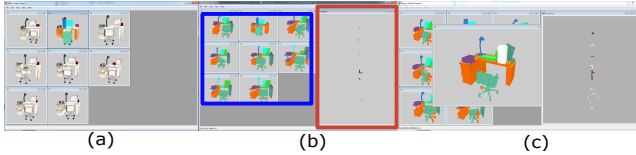


Figure 4: This figure shows the hot intervention mechanism. (a) is the input point sets with manually placed layout in 2nd point set. (b) shows that from the region highlighted by blue rectangle the user can see the instant result of segmentation and from the region highlighted by the red rectangle the user can see the space of latent model(the shape of the centroids of the Gaussian models). (c) shows that the user picks another input point set and add more boxes targeting the incorrect segmentation to further guide the optimization.

5. Experiment and Discussion

5.1. Evaluation for Co-segmentation on Synthetic Data

From the perspective of co-segmentation, we evaluate our algorithm on synthetic data of indoor scenes. To estimate the power of the algorithm we only input layout for one point set in each group for initialization and do not use the hot intervention mechanism. For this evaluation, we think that the color feature is too strong an indication for segmentation in the synthetic data (there is no shadow and lighting variation that will bring in more challenges for segmentation). Using color feature with the bilateral formulation prevents us from doing a fair evaluation of our algorithm, but we need the ground truth of segmentation comes with synthetic data to do the evaluation. For the above reasons, we use only basic formulation for the evaluation of co-segmentation, and no color information is used for optimization. For the estimation, we calculate the intersection over union (IOU) scores for the result segmentation against ground-truth segmentation. We generate three group of synthetic point sets and each group have 13 point sets as inputs. The Figure 5 shows the result of the evalution.

From the evaluation, we want to discuss two observations:

Firstly, for all three groups, the point set with highest IOU score is not the same as the point set equipped with manually placed layout. In other words , the point sets from the 3rd column in Figure 5

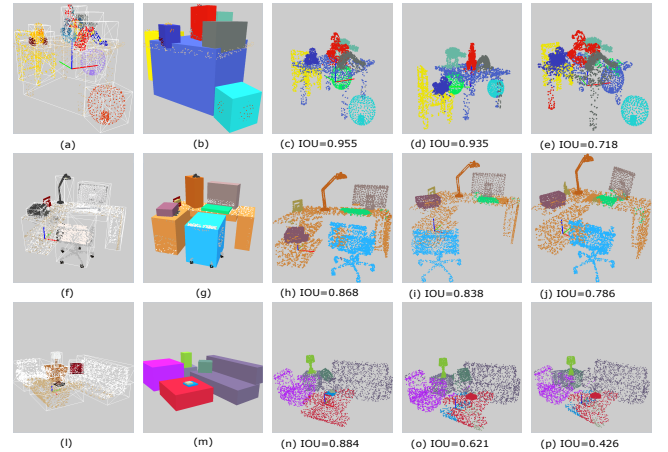


Figure 5: Three rows in the figure shows segmentation evaluations on three groups of synthetic data(child table, office desk, living room). Each group of data have 13 point sets. The first column are examples of point sets for each group of data. The second column are manual placed layout for each group of data. The 3rd column shows the segmentation result with maximum IOU scores in the groups. The 4th column shows the segmentation result with median IOU scores in the groups. The 5th column shows the segmentation result with minimum IOU scores in the groups.

are not the same point sets from 2nd. We believe this is because that the manually placed layout is not accurate respecting to point-wise segmentation. At early iterations of the optimization, the alteration in (18) can serve as a soft constraint to help constraining the shape of object, but in the final iterations the alteration will obstruct the further improvement of segmentation for the correspondent point set.

5.2. Evaluation for Joint Registration on Synthetic Data

In the process of generating synthetic data, we didn't record the groundtruth of the transformation of the

5.3. Test On Real Data

We test our algorithm on a set of real data, Figure 6 shows the result of our test.

5.4. Limitations and Future Work

References

- [CB07] CHEN H., BHANU B.: 3d free-form object recognition in range images using local surface patches. *Pattern Recogn. Lett.* 28, 10 (July 2007), 1252–1262. URL: <http://dx.doi.org/10.1016/j.patrec.2007.02.009>.
- [CLW*14] CHEN K., LAI Y.-K., WU Y.-X., MARTIN R., HU S.-M.: Automatic semantic modeling of indoor scenes from low-quality rgbd data using contextual information. *ACM Trans. Graph.* 33, 6 (Nov. 2014).

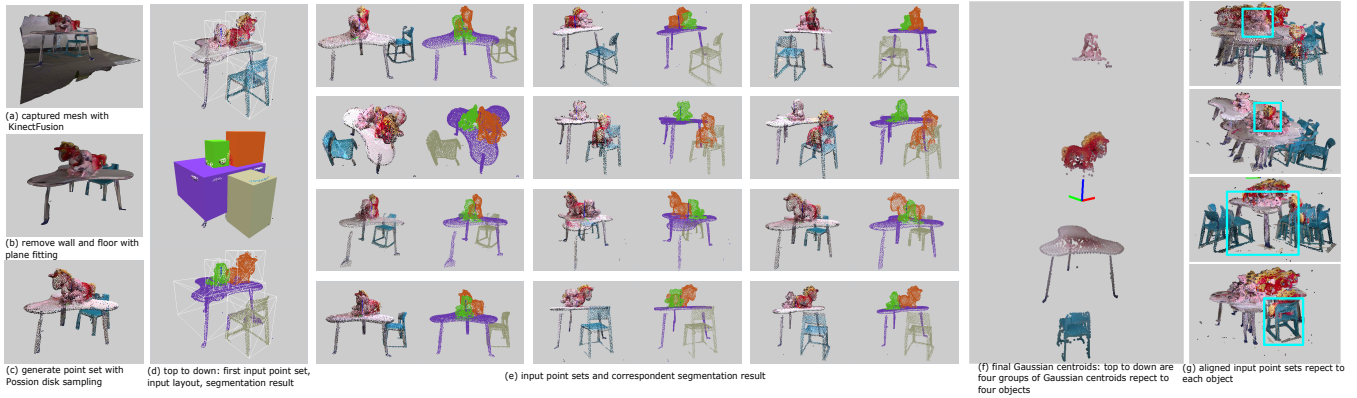


Figure 6: This figure shows our test on a real data. (a)(b)(c) shows how we capture real data and convert to input point set. (d) shows the first input point set, the input layout on it and its segmentation result. (e) shows pairs of other input point sets and corresponding segmentation result. (f) shows the final Gaussian centroids. (g) verifys the registration result by aligning input point sets respecting to each object. The light blue rectangle highlights the object that is aligned together.

- 2014), 208:1–208:12. URL: <http://doi.acm.org/10.1145/2661229.2661239>, doi:10.1145/2661229.2661239. 1, 2
- [DSS12] DEMA M. A., SARI-SARRAF H.: 3d scene generation by learning from examples. In *Multimedia (ISM), 2012 IEEE International Symposium on* (Dec 2012), pp. 58–64. doi:10.1109/ISM.2012.19. 1
- [EKBHP14] EVANGELIDIS G. D., KOUNADEAS-BASTIAN D., HORAUD R., PSARAKIS E. Z.: *A Generative Model for the Joint Registration of Multiple Point Sets*. Springer International Publishing, Cham, 2014, pp. 109–122. URL: http://dx.doi.org/10.1007/978-3-319-10584-0_8, 2, 3, 4, 5
- [FRS*12] FISHER M., RITCHIE D., SAVVA M., FUNKHOUSER T., HANRAHAN P.: Example-based synthesis of 3d object arrangements. *ACM Trans. Graph.* 31, 6 (Nov. 2012), 135:1–135:11. URL: <http://doi.acm.org/10.1145/2366145.2366154>, 1
- [FSN*15] FISHER M., SAVVA M., LI Y., HANRAHAN P., NEISSNER M.: Activity-centric scene synthesis for functional 3d scene modeling. *ACM Trans. Graph.* 34, 6 (Oct. 2015), 179:1–179:13. URL: <http://doi.acm.org/10.1145/2816795.2818057>, doi:10.1145/2816795.2818057. 1
- [IKH*11] IZADI S., KIM D., HILLIGES O., MOLYNEAUX D., NEWCOMBE R., KOHLI P., SHOTTON J., HODGES S., FREEMAN D., DAVISON A., FITZGIBBON A.: Kinectfusion: Real-time 3d reconstruction and interaction using a moving depth camera. In *Proceedings of the 24th Annual ACM Symposium on User Interface Software and Technology* (New York, NY, USA, 2011), UIST ’11, ACM, pp. 559–568. URL: <http://doi.acm.org/10.1145/2047196.2047270>, doi:10.1145/2047196.2047270. 2
- [JGSC15] JIA Z., GALLAGHER A. C., SAXENA A., CHEN T.: 3d reasoning from blocks to stability. *IEEE Transactions on Pattern Analysis and Machine Intelligence* 37, 5 (May 2015), 905–918. doi:10.1109/TPAMI.2014.2359435. 2
- [JV11] JIAN B., VEMURI B. C.: Robust point set registration using gaussian mixture models. *IEEE Transactions on Pattern Analysis and Machine Intelligence* 33, 8 (Aug 2011), 1633–1645. doi:10.1109/TPAMI.2010.223. 2
- [LPR*16] LI Y., PALURI M., REHG J. M., DOLLAR P., UNDEFINED, UNDEFINED, UNDEFINED, UNDEFINED: Unsupervised learning of edges. *2016 IEEE Conference on Computer Vision and*
- Pattern Recognition (CVPR) 00 (2016), 1619–1627. doi:doi.ieeecomputersociety.org/10.1109/CVPR.2016.179. 2
- [LZW*15] LIU Z., ZHANG Y., WU W., LIU K., SUN Z.: Model-driven indoor scenes modeling from a single image. In *Graphics Interface Conference* (2015). 2
- [MS10] MYRONENKO A., SONG X.: Point set registration: Coherent point drift. *IEEE Transactions on Pattern Analysis and Machine Intelligence* 32, 12 (Dec 2010), 2262–2275. doi:10.1109/TPAMI.2010.46. 2
- [MSL*11] MERRELL P., SCHKUFZA E., LI Z., AGRAWALA M., KOLTUN V.: Interactive furniture layout using interior design guidelines. *ACM Trans. Graph.* 30, 4 (July 2011), 87:1–87:10. URL: <http://doi.acm.org/10.1145/2010324.1964982>, 1
- [NXS12] NAN L., XIE K., SHARF A.: A search-classify approach for cluttered indoor scene understanding. *ACM Trans. Graph.* 31, 6 (Nov. 2012), 137:1–137:10. URL: <http://doi.acm.org/10.1145/2366145.2366156>, doi:10.1145/2366145.2366156. 1
- [RKB04] ROTHER C., KOLMOGOROV V., BLAKE A.: “grabcut”: Interactive foreground extraction using iterated graph cuts. In *ACM SIGGRAPH 2004 Papers* (New York, NY, USA, 2004), SIGGRAPH ’04, ACM, pp. 309–314. URL: <http://doi.acm.org/10.1145/1186562.1015720>, doi:10.1145/1186562.1015720. 2
- [TS10] TOMBARI F., STEFANO L. D.: Object recognition in 3d scenes with occlusions and clutter by hough voting. In *2010 Fourth Pacific-Rim Symposium on Image and Video Technology* (Nov 2010), pp. 349–355. doi:10.1109/PSIVT.2010.65. 3
- [TSS16] TANIAI T., SINHA S. N., SATO Y.: Joint recovery of dense correspondence and cosegmentation in two images. In *The IEEE Conference on Computer Vision and Pattern Recognition (CVPR)* (June 2016). 2
- [XCF*13] XU K., CHEN K., FU H., SUN W.-L., HU S.-M.: Sketch2scene: Sketch-based co-retrieval and co-placement of 3d models. *ACM Trans. Graph.* 32, 4 (July 2013), 123:1–123:15. URL: <http://doi.acm.org/10.1145/2461912.2461968>, 1
- [XHS*15] XU K., HUANG H., SHI Y., LI H., LONG P., CAICHEN J., SUN W., CHEN B.: Autoscaning for coupled scene reconstruction and proactive object analysis. *ACM Trans. Graph.* 34, 6 (Oct. 2015), 177:1–177:14. URL: <http://doi.acm.org/10.1145/2816795.2818075>, doi:10.1145/2816795.2818075. 2